Supporting Information

Kumar et al. 10.1073/pnas.1016524108

SI Materials and Methods

Methods for Behavioral Studies. ***Sensorimotor battery.*** A battery of sensorimotor tests was administered to assess balance, strength, coordination, and initiation of movement using previously published methods (1). The battery included ledge and platform tests, which involved timing how long a mouse could remain on an elevated, narrow (0.75 cm wide) Plexiglas ledge or on an elevated small circular wooden platform (1.0 cm thick, 3.0 cm diameter) with rounded edges. A walking initiation test also was performed by timing how long it took a mouse to move out of a small square (21 × 21 cm) outlined on a black tabletop. General coordination and strength were evaluated using the pole, inclined and inverted screen tests. The pole test involved placing a mouse "head up" on top of a finely textured rod (diameter 8 mm; height 55 cm) and timing how long the mouse took to turn and climb down the pole. In the 60° and 90° inclined screen tests mice were placed in the middle of elevated wire mesh grids at differing inclinations (60° or 90°) with their heads oriented down, and the time the mice took to turn and climb to the top of the screen was measured. In the inverted screen test a mouse was placed on the 60° inclined screen which then was inverted, and the time the mouse could remain hanging upside down on the screen before falling was measured. Two trials were administered for each test in the battery, and means were computed for each mouse.

Rotarod. Motor coordination and balance were studied further using a protocol similar to previously published Rotarod test procedures (2), which included three conditions: a stationary rod, a rod that rotated at a constant speed (5 rpm for 60 s maximum), and a rod that rotated at an accelerating speed (5–20 rpm over 1–180 s maximum). The protocol consisted of three training sessions with each session including one stationary rod trial, two constant speed Rotarod trials, and two accelerating Rotarod trials. Sessions were separated by 2 d, and time spent on the rod was used as the dependent variable.

Backward walking. Mice were transferred into the testing room 90 min before the testing sessions and were separated from each other. Walking behavior was recorded by a video camera. All the movies were produced with the written permission of the animal research committees at Washington University and University of Texas Southwestern Medical Center.

Statistical analyses. ANOVA models were used to analyze the data from the sensorimotor battery and Rotarod test. The ANOVA model used for the Rotarod data included one between-subjects variable (Genotype: $Mof^{F/F}/Pcp2\text{-}Cre^{+}$ vs. $Mof^{F/F}/Pcp2\text{-}Cre^{-}$), and two within-subjects variables (Trials and Sessions). For this ANOVA model with repeated measures, the Huynh–Feldt (H-F) adjustment of alpha levels was used for all within-subjects effects containing more than two levels to protect against violations of the sphericity/compound symmetry assumptions underlying the model. Bonferroni correction procedures were used to determine significance when multiple, paired comparisons were conducted (i.e., a P value of $0.05/6 = 0.0083$ was used for the constant speed and accelerating Rotarod tasks).

1. Wozniak DF, et al. (2004) Apoptotic neurodegeneration induced by ethanol in neonatal mice is associated with profound learning/memory deficits in juveniles followed by progressive functional recovery in adults. *Neurobiol Dis* 17:403–414.

2. Grady RM, Wozniak DF, Ohlemiller KK, Sanes JR (2006) Cerebellar synaptic defects and abnormal motor behavior in mice lacking alpha- and beta-dystrobrevin. *J Neurosci* 26: 2841–2851.

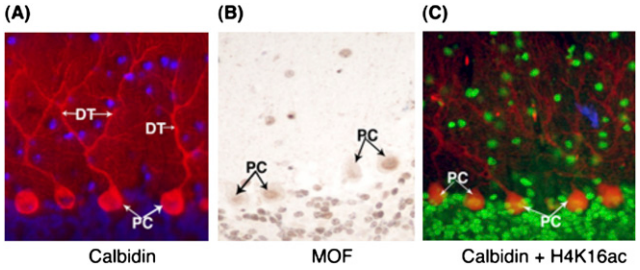

Fig. S1. Section of $Mof^{F/F}/Pcp2\text{-}Cre^{-}$ control mouse cerebellum showing Purkinje cells (PCs) and dendrites (DT). (*A*) Calbindin staining. Arrows indicate PC and DT. (*B*) MOF staining. Arrows indicate intense nuclear HRP staining. (*C*) Calbindin and histone H4 acetylated at lysine 16 (H4K16ac) staining. Arrows indicate greenish-yellow nuclear staining of H4K16ac in PCs.

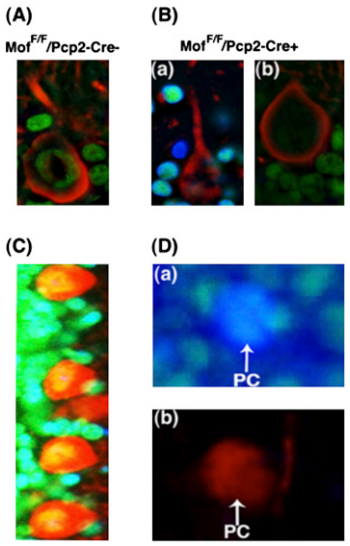

Fig. S2. Calbindin, Mof, and H4K16ac staining in PC. (*A*) PC from 15-d-old *Mof*$^{F/F}$*/Pcp2-Cre*$^{+}$ mouse showing MOF in the nucleus. (*B*) Loss of MOF in PC from 25-d-old (*a*) and 45-d-old *Mof*$^{F/F}$*/Pcp2-Cre*$^{+}$ mice (*b*). (*C*) H4K16ac staining in 15-d-old *Mof*$^{F/F}$*/Pcp2-Cre*$^{+}$ mice. (*D*) Loss of H4K16ac staining in 45-d-old *Mof*$^{F/F}$*/Pcp2-Cre*$^{+}$ mice. (*a*) DAPI-stained and (*b*) Calbindin-stained PC.

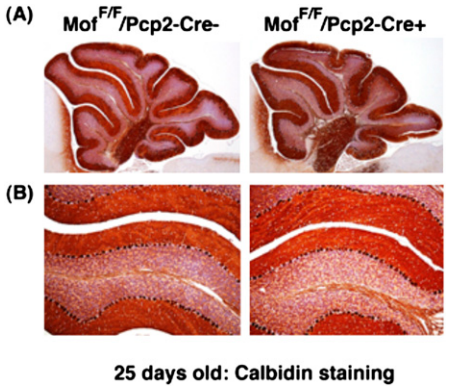

Fig. S3. Calbindin staining of cerebellum sections from 25-d-old mice. (*A*) Whole sagittal section of cerebellum at low magnification. (*B*) A sector of a section at higher magnification. PC morphology and distribution at this age is similar in the cerebellums of *Mof*$^{F/F}$*/Pcp2-Cre*$^{+}$ and *Mof*$^{F/F}$*/Pcp2-Cre*$^{-}$ mice.

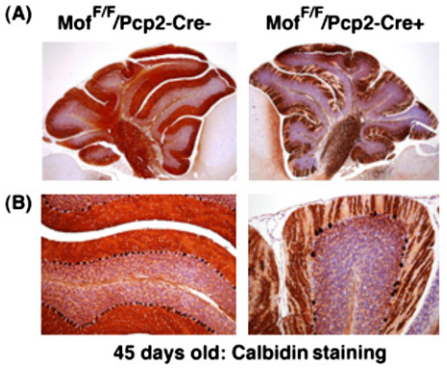

Fig. S4. Calbindin staining of cerebellum sections from 45-d-old mice. (*A*) Whole sagittal section of cerebellum at low magnification. (*B*) A sector of a section at higher magnification. Loss of PC cells is evident in cerebellums of *Mof*$^{F/F}$*/Pcp2-Cre*$^{+}$ mice.

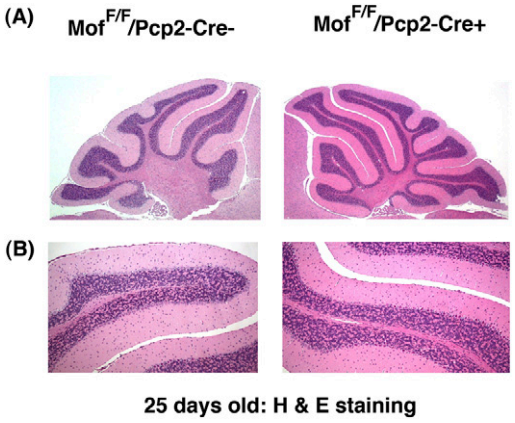

Fig. S5. H&E staining of cerebellum sections from 25-d-old mice. (*A*) Whole sagittal section of cerebellum at low magnification. (*B*) A sector of a section at higher magnification. No major difference in PCs is found in cerebellums of *Mof*$^{F/F}$*/Pcp2-Cre*$^{+}$ and *Mof*$^{F/F}$*/Pcp2-Cre*$^{-}$ mice.

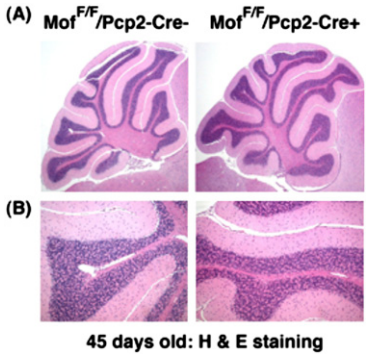

Fig. S6. H&E staining of cerebellum sections from 45-d-old mice. (*A*) Whole sagittal section of cerebellum at low magnification. (*B*) A sector of a section at higher magnification. Pyknotic PCs are found in cerebellums of *Mof*$^{F/F}$*/Pcp2-Cre*$^{+}$ mice.

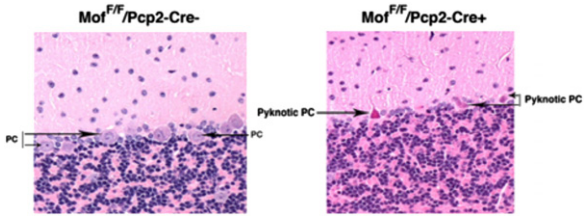

Fig. S7. H&E staining of cerebellum section from 45-d-old mice. Arrows indicate PC in *Mof*$^{F/F}$*/Pcp2-Cre*$^{-}$ mice and pyknotic PC in *Mof*$^{F/F}$*/Pcp2-Cre*$^{+}$ mice.

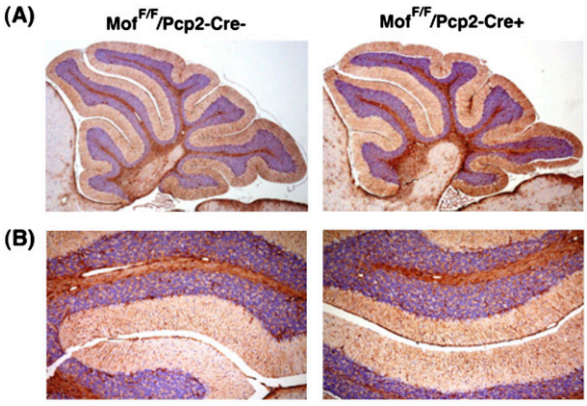

Fig. S8. GFAP staining of cerebellum sections from 25-d-old mice. (*A*) Whole sagittal section of cerebellum at low magnification. (*B*) A section at higher magnification. No difference in GFAP staining is seen in PCs in *Mof*$^{F/F}$*/Pcp2-Cre*$^{-}$ mice and *Mof*$^{F/F}$*/Pcp2-Cre*$^{+}$ mice.

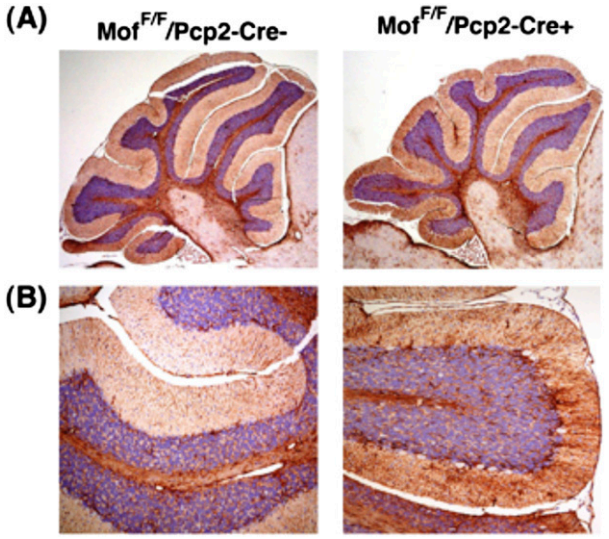

Fig. S9. GFAP staining of a cerebellum section from 45-d-old mice. (*A*) Whole sagittal section of cerebellum at low magnification. (*B*) Section at higher magnification. A difference in GFAP staining is seen in PCs in *Mof*$^{F/F}$*/Pcp2-Cre*$^{-}$ mice and *Mof*$^{F/F}$*/Pcp2-Cre*$^{+}$ mice.

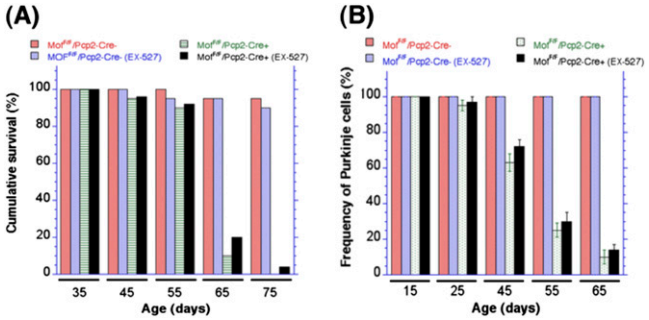

Fig. S10. Effect of MOF and treatment with the histone deacetylase inhibitor EX-527 on survival and PC numbers. (*A*) EX-527 increases cumulative survival of *Mof*$^{F/F}$*/Pcp2-Cre*$^{+}$ mice but not of *Mof*$^{F/+}$*/Pcp2-Cre*$^{-}$ mice. (*B*) EX-527 affects the frequency of PCs in *Mof*$^{F/F}$*/Pcp2-Cre*$^{+}$ mice but not in *Mof*$^{F/F}$*/Pcp2-Cre*$^{-}$ mice.

Movie S1. Mice at postnatal day 35 have difficulty initiating walking. Mice do not move for about 35–40 s. They try to move but are unsuccessful.

Movie S1

Movie S2. A 45-d-old mouse walks both forward (normally) and, occasionally, backward. The backward walking is ~20% of the total walking.

Movie S2

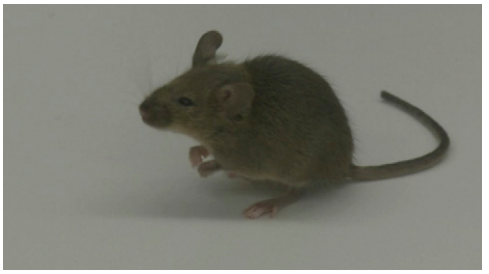

Movie S3. A 55-d-old mouse walking backward.

Movie S3

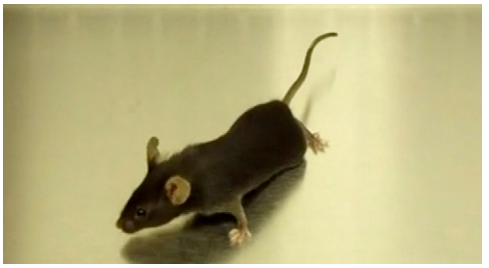

Movie S4. Mice at different ages (older than 55 d) walk only backward.

Movie S4

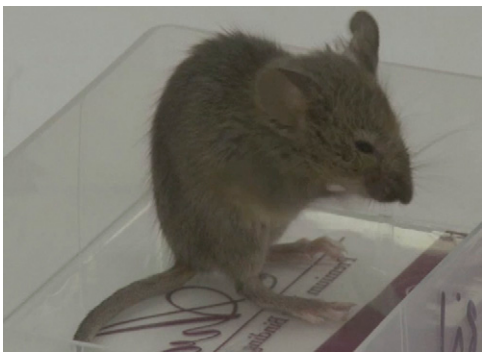

Movie S5. Mice age 65 d with ataxia and head weaving.

Movie S5